1506 *Inorg. Chem.* **2011**, *50*, 1506–1512
DOI: 10.1021/ic1020719

Inorganic Chemistry
Article

Coordination-Driven Self-Assembly of M_3L_2 Trigonal Cages from Preorganized Metalloligands Incorporating Octahedral Metal Centers and Fluorescent Detection of Nitroaromatics

Ming Wang,[†] Vaishali Vajpayee,[‡] Sankarasekaran Shanmugaraju,[§] Yao-Rong Zheng,[†] Zhigang Zhao,[†] Hyunuk Kim,[⊥] Partha Sarathi Mukherjee,*[,§] Ki-Whan Chi,*[,‡] and Peter J. Stang*[,†]

[†]*Department of Chemistry, University of Utah, 315 South 1400 East Salt Lake City, Utah 84112, United States,* [‡]*Department of Chemistry, University of Ulsan, Ulsan 680-749, Republic of Korea,* [§]*Inorganic and Physical Chemistry Department, Indian Institute of Science, Bangalore 560012, India, and* [⊥]*Department of Chemistry, POSTECH, Pohang 690-784, Republic of Korea*

Received October 13, 2010

The design and preparation of novel M_3L_2 trigonal cages via the coordination-driven self-assembly of preorganized metalloligands containing octahedral aluminum(III), gallium(III), or ruthenium(II) centers is described. When tritopic or dinuclear linear metalloligands and appropriate complementary subunits are employed, M_3L_2 trigonal-bipyramidal and trigonal-prismatic cages are self-assembled under mild conditions. These three-dimensional cages were characterized with multinuclear NMR spectroscopy (^{1}H and ^{31}P) and high-resolution electrospray ionization mass spectrometry. The structure of one such trigonal-prismatic cage, self-assembled from an arene ruthenium metalloligand, was confirmed via single-crystal X-ray crystallography. The fluorescent nature of these prisms, due to the presence of their electron-rich ethynyl functionalities, prompted photophysical studies, which revealed that electron-deficient nitroaromatics are effective quenchers of the cages' emission. Excited-state charge transfer from the prisms to the nitroaromatic substrates can be used as the basis for the development of selective and discriminatory turn-off fluorescent sensors for nitroaromatics.

Introduction

Three-dimensional (3D) supramolecular entities are ubiquitous throughout nature and account for various biological functions. For example, viral capsids are precisely assembled cages comprised of protein subunits and serve the biological role of nucleic acid storage.[1] In the past 2 decades, weak noncovalent and dative metal−ligand interactions have been exploited using appropriately designed molecular subunits in a predictive manner to construct aesthetically appealing abiological 3D self-assemblies.[2] This approach has also provided access to functional materials with a wide range of desirable structural and dynamic properties.[3] The construction of functional supramolecular architectures possessing tailor-made properties, such as molecular recognition,[4] host−guest chemistry,[5] and supramolecular catalysis[3f,6] has become the focus of modern metallosupramolecular chemistry. Transition-metal-mediated, coordination-driven self-assembly has emerged as a useful synthetic tool to access such species.

*To whom correspondence should be addressed. E-mail: psm@ipc.iisc.ernet.in (P.S.M.), kwchi@mail.ulsan.ac.kr (K.-W.C.), stang@chem.utah.edu (P.J.S.).

(1) (a) Cann, A. J. *Principles of Molecular Virilogy*; Academic Press: San Diego, 1993. (b) Uchida, M.; Klem, M. T.; Allen, M.; Suci, P.; Flenniken, M.; Gillitzer, E.; Varpness, Z.; Liepold, L. O.; Young, M.; Douglas, T. *Adv. Mater.* **2007**, *19*, 1025.

(2) (a) Stang, P. J.; Olenyuk, B. *Acc. Chem. Res.* **1997**, *30*, 502. (b) Leininger, S.; Olenyuk, B.; Stang, P. J. *Chem. Rev.* **2000**, *100*, 853. (c) Holliday, B. J.; Mirkin, C. A. *Angew. Chem., Int. Ed.* **2001**, *40*, 2022. (d) Seidel, S. R.; Stang, P. J. *Acc. Chem. Res.* **2002**, *35*, 972. (e) Fujita, M.; Tominaga, M.; Hori, A.; Therrien, B. *Acc. Chem. Res.* **2005**, *38*, 369. (f) Oliver, C. G.; Ulman, P. A.; Wiester, M. J.; Mirkin, C. A. *Acc. Chem. Res.* **2008**, *41*, 1618. (g) De, S.; Mahata, K.; Schmittel, M. *Chem. Soc. Rev.* **2010**, *39*, 1555.

(3) (a) Fiedler, D.; Leung, D. H.; Bergman, R. G.; Raymond, K. N. *Acc. Chem. Res.* **2005**, *38*, 349. (b) Northrop, B. H.; Yang, H.-B.; Stang, P. J. *Chem. Commun.* **2008**, 5896. (c) Northrop, B. H.; Chercka, D.; Stang, P. J. *Tetrahedron* **2008**, *64*, 11495. (d) Parkash, M. J.; Lah, M. S. *Chem. Commun.* **2009**, 3326. (e) Raymond, K. N. *Nature* **2009**, *460*, 585. (f) Pluth, M. D.; Bergman, R. G.; Raymond, K. N. *Acc. Chem. Res.* **2009**, *42*, 1650. (g) Lee, J.; Farha, O. K.; Roberts, J.; Scheidt, K. A.; Nguyen, S. T.; Hupp, J. T. *Chem. Soc. Rev.* **2009**, *38*, 1450.

(4) (a) Resendiz, M. J. E.; Noveron, J. C.; Disteldorf, H.; Fischer, S.; Stang, P. J. *Org. Lett.* **2004**, *6*, 651. (b) Lin, R.; Yip, J. H.; Zhang, K.; Koh, L. L.; Wong, K. Y.; Ho, K. P. *J. Am. Chem. Soc.* **2004**, *126*, 15852. (c) Bar, A. K.; Chakrabarty, R.; Mostafa, G.; Mukherjee, P. S. *Angew. Chem., Int. Ed.* **2008**, *47*, 8455. (d) Malina, J.; Hannon, M. J.; Brabec, V. *Nucleic Acids Res.* **2008**, *36*, 3630.

(5) (a) Yoshizawa, M.; Klosterman, J. K.; Fujita, M. *Angew. Chem., Int. Ed.* **2009**, *48*, 3418. (b) He, Q.-T.; Li, X.-P.; Liu, Y.; Yu, Z.-Q.; Wang, W.; Su, C.-Y. *Angew. Chem., Int. Ed.* **2009**, *48*, 6156. (c) Mal, P.; Breiner, B.; Rissanen, K.; Nitschke, J. R. *Science* **2009**, *324*, 1697. (d) Clever, G. H.; Tashiro, S.; Shionoya, M. *Angew. Chem., Int. Ed.* **2009**, *48*, 7010. (e) Liao, P.; Langloss, B. W.; Johnson, A. M.; Knudsen, E. R.; Tham, F. S.; Julian, R. R.; Hooley, R. J. *Chem. Commun.* **2010**, *46*, 4932. (f) Peinador, C.; Pía, E.; Blanco, V. C.; García, M. D.; Quintela, J. M. *Org. Lett.* **2010**, *12*, 1380.

 Published on Web 01/07/2011

For example, hydrophobic or fluorous nanophases were accessed by endofunctionalized $M_{12}L_{24}$ molecular spheres assembled by this route.[7a] Additionally, similarly formed chiral metal−organic tetrahedral cages have separated racemic mixtures with high enantioselectivity.[7g]

To date, the directional bonding approach for the coordination-driven self-assembly of 3D metallosupramolecules has proven quite successful and focuses on the use of rigid, organic ligands encoded with information on directionality and angularity. More recently, interest in the application of preorganized metallocomplexes to direct the coordination-driven self-assembly and the preparation of metallosupramolecules has increased.[8−11] Self-assemblies constructed from such building blocks can introduce unique characteristics such as magnetic[8d] or photophysical properties and chiral centers,[8e] while avoiding the time-consuming and expensive multistep syntheses required to install these attributes via conventional synthetic pathways. We have previously shown that two-dimensional polygons can be constructed from the coordination-driven self-assembly of metalloligands.[12] For example, a [5 + 5] pentagon was prepared from 108° metal carbonyl dipyridine ligands,[12] and [3 + 3] hexagons and [2 + 2] rhomboids containing cobalt carbonyl motifs have been prepared via supramolecule-to-supramolecule transformations of ethynyl-functionalized building blocks.[12b] We now report on the extension of this approach to 3D assemblies.

Square-planar palladium(II) and platinum(II) metals have been exploited for their structural rigidity in the synthesis of several discrete structures of predefined shapes and sizes.[2,3] Octahedral metal ions are known to be less predictable for the construction of defined discrete structures. However, the construction of discrete metallosupramolecules via the self-assembly of transition-metal complexes with octahedral geometries is a growing field because of the versatile properties expected in the presence of such metal ions.[8,11,12] The application of octahedral and square-planar metal ions together with the generation of discrete and defined structures has not been well explored. In a continuation of our investigation into the scope and diversity of functional metallosupramolecules, herein we present M_3L_2 3D trigonal-bipyramidal cages that are assembled from preorganized metalloligands containing octahedral aluminum(III) and gallium(III) centers (Scheme 1) in combination with platinum(II) acceptors. M_3L_2 cages represent the simplest 3D supramolecular structures[13] and can be assembled by the combination of two tritopic subunits and three ditopic tectons.[14] To further explore the self-assembly of M_3L_2 cages in a complementary way using octahedral metalloligands, we report the reactions of octahedral ruthenium(II) metal-containing

Scheme 1. Coordination-Driven Self-Assembly of M_3L_2 Cages from Metalloligands with Octahedral Metal Centers

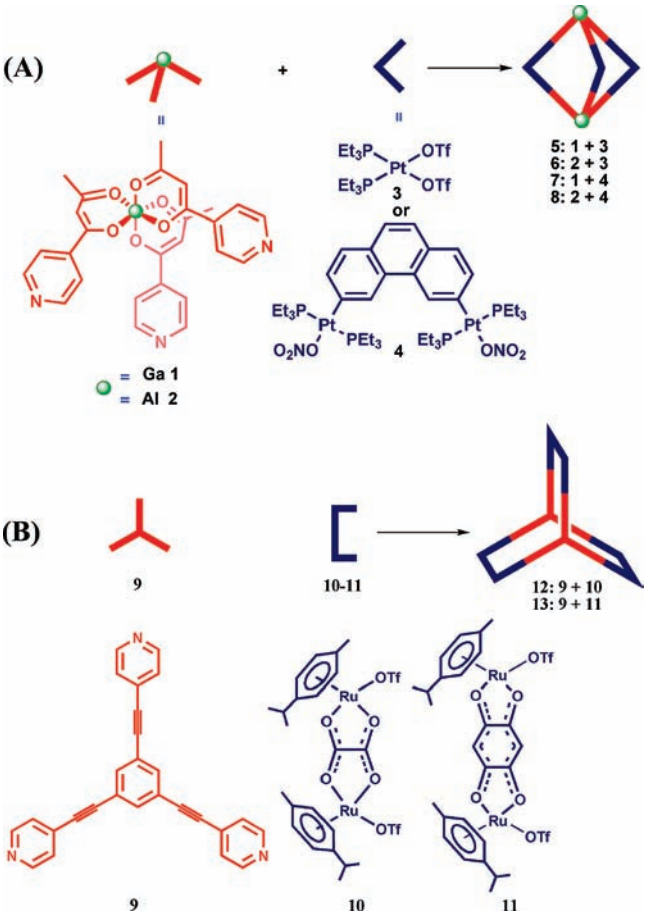

(6) (a) Merlau, M. L.; Mejia, M. D. P.; Nguyen, S. T.; Hupp, J. T. *Angew. Chem., Int. Ed.* **2001**, *40*, 4239. (b) Masar, M. S.; Gianneschi, N. C.; Oliveri, C. G.; Stern, C. L.; Nguyen, S. T.; Mirkin, C. A. *J. Am. Chem. Soc.* **2007**, *129*, 10149. (c) Lee, S. J.; Cho, S. H.; Mulfort, K. L.; Tiede, D. M.; Hupp, J. T.; Nguyen, S. T. *J. Am. Chem. Soc.* **2008**, *130*, 16828. (d) Ulmann, P. A.; Braunschweig, A. B.; Lee, O. S.; Wiester, M. J.; Schatz, G. C.; Mirkin, C. A. *Chem. Commun.* **2009**, 5121.

(7) (a) Yoshizawa, M.; Tamura, M.; Fujita, M. *Science* **2006**, *312*, 251. (b) Ghosh, K.; Yang, H.-B.; Northrop, B. H.; Lyndon, M. M.; Zheng, Y.-R.; Muddiman, D. C.; Stang, P. J. *J. Am. Chem. Soc.* **2008**, *130*, 5320. (c) Yang, H.-B.; Ghosh, K.; Zhao, Y.; Northrop, B. H.; Lyndon, M. M.; Muddiman, D. C.; White, H. S.; Stang, P. J. *J. Am. Chem. Soc.* **2008**, *130*, 839. (d) Ghosh, K.; Hu, J.-M.; White, H. S.; Stang, P. J. *J. Am. Chem. Soc.* **2009**, *131*, 6695. (e) Zhao, L.; Ghosh, K.; Zheng, Y.-R.; Stang, P. J. *J. Org. Chem.* **2009**, *74*, 8516. (f) Suzuki, K.; Takao, K.; Sato, S.; Fujita, M. *J. Am. Chem. Soc.* **2010**, *132*, 2544. (g) Liu, T.; Liu, Y.; Xuan, W.; Cui, Y. *Angew. Chem., Int. Ed.* **2010**, *49*, 4121. (h) Zheng, Y.-R.; Ghosh, K.; Yang, H.-B.; Stang, P. J. *Inorg. Chem.* **2010**, *49*, 4747.

(8) (a) Vreshch, V. D.; Lysenko, A. B.; Chernega, A. N.; Howard, J. A. K.; Krautscheid, H.; Sieler, J.; Domasevitch, K. V. *Dalton Trans.* **2004**, 2899. (b) Müller, I. M.; Möller, D. *Angew. Chem., Int. Ed.* **2005**, *44*, 2969. (c) Tidmarsh, I. S.; Faust, T. B.; Adams, H.; Harding, L. P.; Russo, L.; Clegg, W.; Ward, M. D. *J. Am. Chem. Soc.* **2008**, *130*, 15167. (d) Duriska, M. B.; Neville, S. M.; Moubaraki, B.; Cashion, J. A.; Halder, G. J.; Chapman, K. W.; Balde, C.; Letard, J. F.; Murray, K. S.; Kepert, C. J.; Batten, S. R. *Angew. Chem., Int. Ed.* **2009**, *48*, 2549. (e) Wu, H.-B.; Wang, Q.-M. *Angew. Chem., Int. Ed.* **2009**, *48*, 7343.

(9) (a) Benkstein, K. D.; Hupp, J. T.; Stern, C. L. *J. Am. Chem. Soc.* **1998**, *120*, 12982. (b) Manimaran, B.; Thanasekaran, P.; Rajendran, T.; Liao, R.-T.; Liu, Y.-H.; Lee, G.-H.; Peng, S.-M.; Rajagopal, S.; Lu, K.-L. *Inorg. Chem.* **2003**, *42*, 4795.

(10) (a) Han, Y.-F.; Jia, W.-G.; Yu, W.-B.; Jin, G.-X. *Chem. Soc. Rev.* **2009**, *38*, 3419. (b) Therrien, B. *Eur. J. Inorg. Chem.* **2009**, 2445.

(11) (a) Yan, H.; Suss-Fink, G.; Neels, A.; Stoeckli-Evans, H. *Dalton Trans.* **1997**, 4345. (b) Therrien, B.; Suss-Fink, G.; Govindaswamy, P.; Renfrew, A. K.; Dyson, P. J. *Angew. Chem., Int. Ed.* **2008**, *47*, 3773. (c) Govindaswamy, P.; Suss-Fink, G.; Therrien, B. *Organometallics* **2007**, *26*, 915. (d) Mattson, J.; Govindaswamy, P.; Renfrew, A. K.; Dyson, P. J.; Stepnicka, P.; Suss-Fink, G.; Therrien, B. *Organometallics* **2009**, *28*, 4350. (e) Mattsson, J.; Govindaswamy, P.; Furrer, J.; Sei, Y.; Yamaguchi, K.; Suess-Fink, G.; Therrien, B. *Organometallics* **2008**, *27*, 4346.

(12) (a) Zhao, L.; Ghosh, K.; Zheng, Y.-R.; Lyndon, M. M.; Williams, T. I.; Stang, P. J. *Inorg. Chem.* **2009**, *48*, 5590. (b) Zhao, L.; Northrop, B. H.; Stang, P. J. *J. Am. Chem. Soc.* **2008**, *130*, 11886.

(13) (a) Ikeda, A.; Yoshimura, M.; Udzu, H.; Fukuhara, C.; Shinkai, S. *J. Am. Chem. Soc.* **1999**, *121*, 4296. (b) Claessens, C. G.; Torres, T. *Chem. Commun.* **2004**, 1298.

(14) (a) Radhakrishnan, U.; Schweiger, M.; Stang, P. J. *Org. Lett.* **2001**, *3*, 3141. (b) Yang, H.-B.; Ghosh, K.; Das, N.; Stang, P. J. *Org. Lett.* **2006**, *8*, 3991. (c) Yang, H.-B.; Ghosh, K.; Arif, A. M.; Stang, P. J. *J. Org. Chem.* **2006**, *71*, 9464. (d) Yang, H.-B.; Ghosh, K.; Northrop, B. H.; Stang, P. J. *Org. Lett.* **2007**, *9*, 1561.

bidentate acceptors with tridentate pyridyl donor 1,3,5-tris-(4-pyridylethynyl)benzene to afford M_3L_2 trigonal prisms.

In this paper, octahedral complexes **1** and **2**, prepared from 4-pyridylbutane-1,3-dione and cationic gallium(III) and aluminum(III), respectively, were employed as tritopic ligands for the assembly of trigonal-bipyramidal cages (Scheme 1, A). Treatment of cationic gallium(III) or aluminum(III) with 4- pyridylbutane-1,3-dione resulted in coordination of the latter's β-diketone moiety, poising the three pyridine groups of **1** or **2** to subsequently bind additional metal centers. Furthermore, the pyridine rings were oriented orthogonally to one another because of the octahedral coordination environment about the metal centers, permitting 3D growth.[8a,e] Thus, when octahedral metal-containing donors **1** and **2** were combined with 90° or 60° platinum acceptors, M_3L_2-type heterometallic trigonal-bipyramidal cages were formed. In a complementary approach, dinuclear half-sandwich octahedral ruthenium(II) arene acceptors **10** and **11**[15,16] were combined with 1,3,5-tris(4-pyridylethynyl)benzene **9** to assemble M_3L_2 trigonal-prismatic cages (Scheme 1, B). The ethynyl groups built into ligand **9** impart electron-rich and fluorescent properties to cages **12** and **13**. Using UV−Vis and fluorescence emission spectral analysis, we investigated the host−guest properties of cages **12** and **13** with electron-deficient nitroaromatics. Upon the addition of nitroaromatics, the emission of **12** and **13** was quenched, demonstrating the utility of these cages for the development of selective and discriminatory fluorescence sensors for nitroaromatics.

Results and Discussion

Construction of M_3L_2 Heterometallic Trigonal-Bipyramidal Cages. The preparation of heterometallic trigonal-bipyramidal cages **5** and **6** was achieved by the [2 + 3] self-assembly of metalloligands **1** and **2**, respectively, with the 90° platinum acceptor **3**. Upon the addition of a CD_2Cl_2 solution of ligand **1** or **2** into 1.5 equiv of **3** in CD_3NO_2, **5** and **6** were obtained after 5 h of stirring at room temperature. Similarly, for the self-assembly of **7** and **8**, metalloligands **1** and **2** were treated with the 60° acceptor **4** in an acetone-d_6 and D_2O (1:1, v/v) solution for 15 h at 65 °C. $^{31}P\{^1H\}$ and ^1H NMR multinuclear analysis of the reaction mixtures revealed the formation of single, discrete species with high symmetry. The $^{31}P\{^1H\}$ NMR spectra of self-assemblies **5**−**8** display single, sharp singlets with concomitant ^{195}Pt satellites (−1.4 ppm for **5**, −0.3 ppm for **6**, 14.2 ppm for **7**, and 11.8 ppm for **8**) shifted upfield [$\Delta\delta$ (ppm) = 14.0 for **5**, 12.9 for **6**, 4.1 for **7**, and 6.5 for **8**] relative to starting platinum acceptor **3** or **4** [Figures 1A and S1 in the Supporting Information (SI)]. Compared to their signals before self-assembly, the resonances of the α and β protons of the pyridine rings show significant downfield shifts in the ^1H NMR spectra of these trigonal-bipyramidal cages (Figures 1B and S2−S4 in the SI), due to the loss of electron density upon coordination to platinum. It is also notable that the doublets at

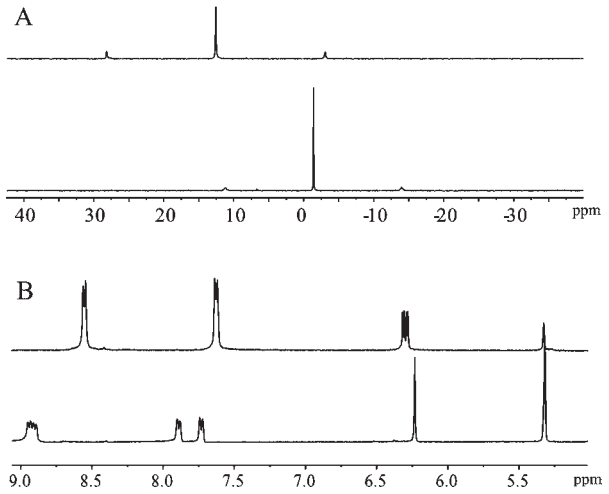

Figure 1. (A) $^{31}P\{^1H\}$ NMR spectra of the starting 90° platinum acceptor **3** (top) and the trigonal-bipyramidal cage **5** (bottom). (B) Partial ^1H NMR (300 MHz, 298 K) of donor **1** (top) and trigonal-bipyramidal cage **5** (bottom). All NMR spectra were recorded in CD_2Cl_2/CD_3NO_2 (2:1, v/v).

8.65 and 7.75 ppm, which were ascribed to the α and β protons of the pyridine ring in the coordinated cages of **5** and **6**, split into pairs of doublets. A similar split was observed for the doublet at 8.70 ppm corresponding to the α protons of the pyridine rings of **7** and **8** (Figures S2−S4 in the SI). These results can be explained by the hindered rotation of the pyridine rings upon coordination to platinum, consistent with our previous reports.[15] The sharp NMR signals in both the ^{31}P and ^1H NMR spectra, along with the solubility of these species, ruled out the formation of oligomers in solution.

Further proof for the trigonal-bipyramidal structures of **5**−**8** was obtained using electrospray ionization mass spectrometry (ESI-MS). The ESI-MS spectrum of **5** exhibited two charged states at m/z 1500.2 and 950.8, corresponding to $[M - 2OTf]^{2+}$ and $[M - 3OTf]^{3+}$, respectively. For assembly **6**, two charged states at m/z 1457.3 and 654.7 were assigned to $[M - 2OTf]^{2+}$ and $[M - 4OTf]^{4+}$, respectively. Charged states at m/z 1473.4 (**7**) and 1089.6 (**7**) and m/z 1445.5 (**8**) and 1068.6 (**8**) were observed to correspond with $[M - 3NO_3]^{3+}$ and $[M - 4NO_3]^{4+}$ for these final two cages, **7** and **8**. These peaks were isotopically resolved and in good agreement with the calculated theoretical distributions (Figures 2 and S5 in the SI).

Although X-ray structural information was elusive for the trigonal-bipyramidal cages, the sizes and shapes of **5** and **7** were ascertained from the results of MM2 force-field simulations (Figure 3). The calculated inner-cavity diameter of these cages was ca. 1.3 nm for **5** and ca. 1.8 nm for **7**.

Trigonal-Prismatic Cages Self-Assembled from Half-Sandwich Ruthenium(II) Metalloligands. Trigonal-prismatic cages **12** and **13** were obtained by [2 + 3] self-assembly of the tritopic planar donor **9** with half-sandwich arene ruthenium(II) metalloligands **10** and **11**, respectively. A nitromethane solution containing **9** was added to a methanol solution of **10** or **11** in a 2:3 ratio and allowed to stir at room temperature for 4 h. Upon the addition of diethyl ether into the concentrated reaction mixtures, **12** and **13** were precipitated as yellow and red-wine crystalline solids, respectively. The trigonal-prismatic structures of **12** and **13** were confirmed

(15) (a) Tarkanyi, G.; Jude, H.; Palinkas, G.; Stang, P. J. *Org. Lett.* **2005**, *7*, 4971. (b) Caskey, D. C.; Yamamoto, T.; Addicott, C.; Shoemaker, R. K.; Vacek, J.; Hawkridge, A. M.; Muddiman, D. C.; Kottas, G. S.; Michl, J.; Stang, P. J. *J. Am. Chem. Soc.* **2008**, *130*, 7620. (c) Vacek, J.; Caskey, D. C.; Horinek, D.; Shoemaker, R. K.; Stang, P. J.; Michl, J. *J. Am. Chem. Soc.* **2008**, *130*, 7629. (d) Zhao, L.; Ghosh, K.; Zheng, Y.-R.; Stang, P. J. *J. Org. Chem.* **2009**, *74*, 8516.

(16) Han, Y.-F.; Lin, Y.-J.; Jia, W.-G.; Wang, G.-L.; Jin, G.-X. *Chem. Commun.* **2008**, 1807.

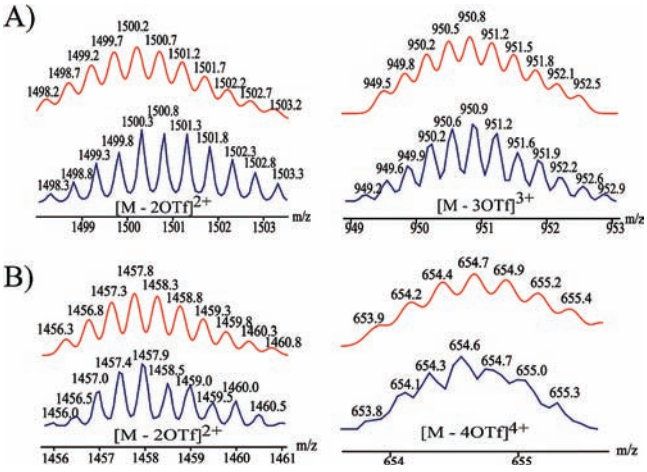

Figure 2. Calculated (red) and experimental (blue) ESI-MS spectra of trigonal-bipyramidal cages **5** (A) and **6** (B).

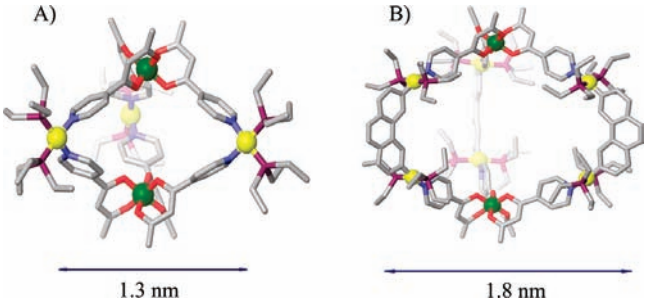

Figure 3. Proposed structure of the heterometallic, trigonal-bipyramidal cages **5** (A) and **7** (B) as obtained by MM2 force-field simulation.

by NMR and high-resolution ESI-MS analysis. The molecular structure of **12** was further elucidated by single-crystal X-ray diffraction using synchrotron radiation. The ^{1}H NMR spectra of **12** and **13** exhibit two doublets (δ 8.21 and 7.61 for **12** and δ 8.45 and 7.65 for **13**), assigned to the pyridine protons of the self-assemblies. Additionally, sharp singlets at δ 7.78 (**12**) and 7.84 (**13**) were observed for the 2, 4, and 6 protons of the central aromatic ring of **9** and two doublets for the *p*-cymene moiety were observed at δ 6.11 and 5.96 for **12** and δ 6.21 and 6.01 for **13** (Figure S6 in the SI). The assignment of trigonal-prismatic structures to **12** and **13** was also supported by ESI-MS analysis (Figure 4). Charged states at m/z 1517.0 (**12**), 961.7 (**12**), 1592.8 (**13**), and 1011.9 (**13**) were observed, corresponding to $[M - 2OTf]^{2+}$ and $[M - 3OTf]^{3+}$. These peaks were isotopically resolved and in good agreement with the calculated theoretical distributions. After anions were exchanged from a triflate to a perchlorate, a single crystal of **12** suitable for X-ray analysis was obtained by the slow vapor diffusion of diethyl ether into a dichloromethane/methanol solution of **12** (Table S1 in the SI). As shown in Figure 5, the two tritopic ligands are arranged face-to-face, coordinated to three arene ruthenium metalloligands to give a trigonal-prismatic structure with a height of approximately 7 Å and a distance of about 24 Å between the edges. Inspection of the crystal packing reveals that **12** has a one-dimensional columnar structure along the α axis. Discrete trigonal prisms stack to give favorable $\pi-\pi$ interactions with a 60° rotation between cages and an intermolecular spacing

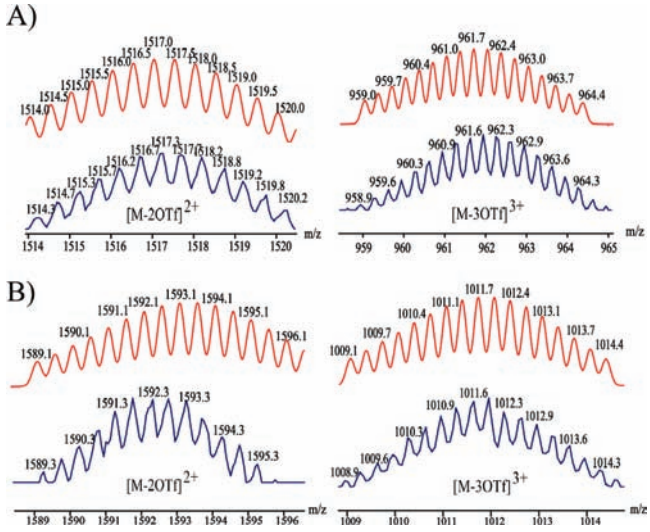

Figure 4. Calculated (red) and experimental (blue) ESI-MS spectra of trigonal-prismatic cages **12** (A) and **13** (B).

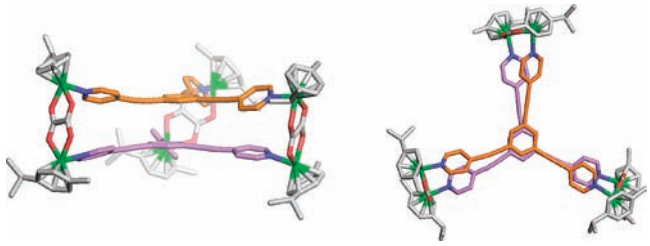

Figure 5. X-ray structures of the trigonal-prismatic cage **12**: side view (left) and top view (right). Color code: green, Ru; red, O; blue, N. H atoms, counteranions, and solvent molecules are omitted for clarity.

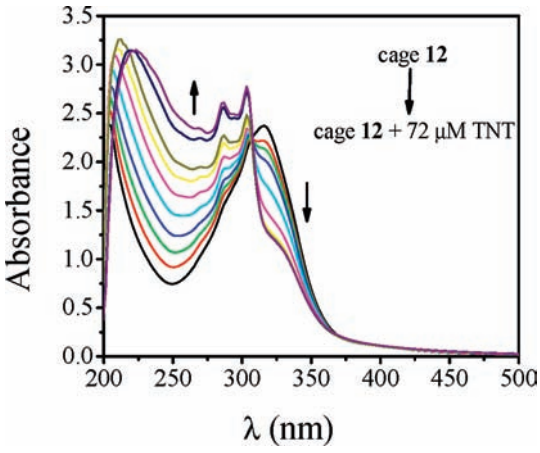

Figure 6. UV−Vis spectra of **12** (1.0×10^{-5} M solution in methanol) in the presence of TNT (from 0 to 72 μM).

of 3.4 Å. The interstitial sites of the crystal structures for **12** are occupied by perchlorate counteranions and solvent molecules.

Photophysical Studies of Trigonal-Prismatic Cages 12 and 13: Fluorescent Detection of Nitroaromatics. Cages **12** and **13** (0.01 mM in MeOH) exhibit strong bands at λ = 310 nm for **12** and λ = 315 nm for **13**, which are attributed to intra/intermolecular $\pi-\pi^*$ transitions. The absorption features of **12** exhibit dynamic behavior in the presence of nitroaromatics. The incorporation of electron-rich ethynyl moieties rendered cage **12** fluorescent; therefore, electronic

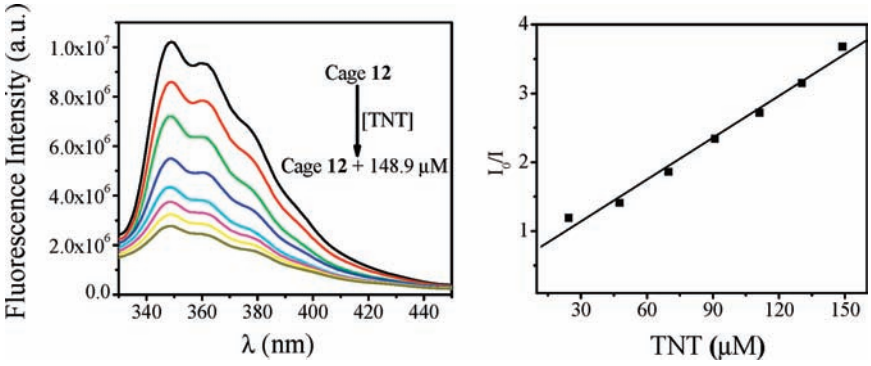

Figure 7. Fluorescence spectra of **12** (1.0×10^{-6} M in methanol) in the presence of TNT (from 0 to 175 μM), $\lambda_{ex} = 280$ nm (left); Stern−Volmer plot of the fluorescence quenching of **12** by TNT. The fluorescence intensity was monitored at 350 nm (right).

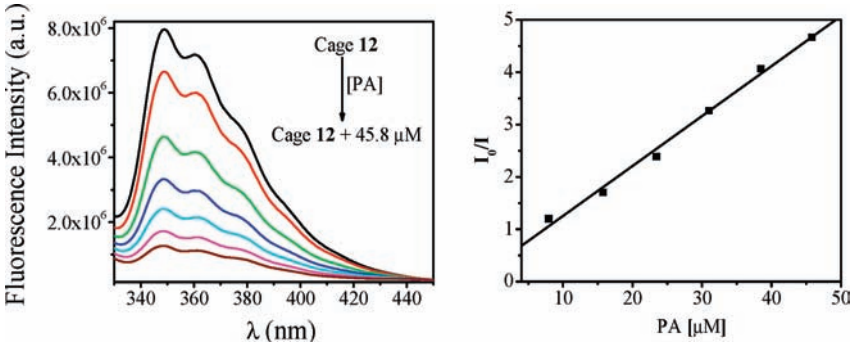

Figure 8. Fluorescence quenching of **12** by PA (left) and the corresponding Stern−Volmer plot (right). Fluorescence spectra were recorded using solutions of **12** (1×10^{-6} M) in methanol monitored at 350 nm.

variations were monitored upon the addition of electron-deficient nitroaromatics. When trinitrotoluene (TNT) was added to a solution of **12** (1.0×10^{-5} M in methanol), significant absorption changes in the UV−Vis spectra were observed, as shown in Figure 6. Upon the addition of TNT, the strong absorption at 315 nm decreases in intensity while a new absorption at 250 nm gradually increases, reaching a maximum at a TNT concentration of 72 μM. The well-anchored isosbestic point at 306 nm in the absorption spectra of **12** upon TNT addition indicates the formation of a stable complex between **12** and TNT.

Solutions of **12** and **13** (1.0×10^{-6} M in methanol) are emissive when excited at 280 nm, the spectra of which exhibit three bands with wavelengths of 349, 361, and 380 nm (Figure 7). The quantum yields of **12** and **13** were determined to be 0.12 and 0.22, respectively, relative to that of anthracene (Table 2 in the SI). The emission spectra were sensitive to the addition of nitroaromatics, which quenched the emission of the self-assemblies significantly. The fluorescence intensity of **12** decreased 70% in the presence of 148.9 μM TNT (Figure 7, left). The ratio of the fluorescence intensities, I_0/I (monitored at 350 nm), where I and I_0 represent the fluorescence intensity of **12** with and without TNT, respectively, shows a linear response to the TNT concentration in the range of 0−150 μM (Figure 7, right). The Stern−Volmer constant K_{sv} was determined to be 2.1×10^4 M^{-1} by fitting the linear plot to the Stern−Volmer equation $I_0/I = 1 + K_{sv}[TNT]$. The stiochiometry and binding constant of TNT/cage **12** were determined to be 5:1 and 4.91×10^4 M^{-1}, respectively (Figures S7 and S8 in the SI). Notably, the addition of 45.8 μM picric acid (PA) quenched the fluorescence of **12** completely compared to TNT under the same conditions (Figure 8). In this case, the Stern−Volmer constant was determined to be 1.0×10^5 M^{-1}. This phenomenon can be explained by the electron-deficient nature of PA relative to TNT, leading to a stronger electron transfer and ultimately more efficient quenching.[17,18]

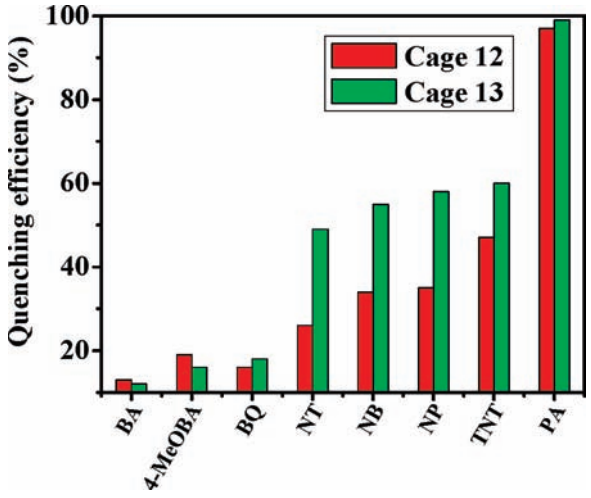

Figure 9. Selective fluorescent detection of nitroaromatics using coordinated trigonal-prismatic cages **12** and **13**. The fluorescence intensities of solutions of **12** and **13** (1.0×10^{-6} M in methanol) were monitored at 350 nm.

(17) (a) Ghosh, S.; Gole, B.; Bar, A. K.; Mukherjee, P. S. *Organometallics* **2009**, *28*, 4288. (b) Ghosh, S.; Mukherjee, P. S. *Organometallics* **2008**, *27*, 316.

(18) (a) Toal, S. J.; Trogler, W. C. *J. Mater. Chem.* **2006**, *16*, 2871. (b) Swager, T. M. *Acc. Chem. Res.* **2008**, *41*, 1181. (c) Germain, M. E.; Knapp, M. J. *Chem. Soc. Rev.* **2009**, *38*, 2543.

When a variety of aromatic compounds such as benzoic acid, 4-methoxybenzoic acid, 1,4-benzoquinone, 4-nitrotoluene, nitrobenzene, 4-nitrophenol, TNT, and PA were added to solutions of **12** or **13**, only the nitroaromatics efficiently quenched the fluorescence emission, as shown in Figure 9. This result is consistent with the expected mode of $\pi-\pi$ interactions, in which electron-deficient nitroaromatics act as fluorescence quenchers either via excited-state electron transfer from the electron-rich prismatic cage **12** or **13** or by charge-transfer complex formation.

Conclusion

We present in this paper the construction of M_3L_2 trigonal cages via the coordination-driven self-assembly of preorganized metalloligands containing octahedral metal centers. Tritopic pyridine ligands incorporating aluminum or gallium, in which the coordination sites for self-assembly are controlled by the metal's octahedral coordination environment, were assembled with appropriately angled (60° or 90°) platinum acceptors and afforded novel heterometallic trigonal-bipyramidal cages. Two trigonal-prismatic cages were successfully constructed from the self-assembly of an electron-rich, planar donor, 1,3,5-tris(4-pyridylethynyl)benzene (**9**) with dinuclear ruthenium arene metalloligands, with the former possessing two octahedral ruthenium centers capped by *p*-*i*PrC_6H_4Me and bridged by either oxalate ($C_2O_4^{2-}$) or 2,5-dihydroxy-1,4-benzoquinonato ($C_6H_2O_4^{2-}$). Furthermore, we have demonstrated that the self-assembly of building blocks possessing ethynyl functionalities can endow the 3D cages with interesting properties, such as increased electron density and fluorescence. The efficient electron transfer from the self-assembled trigonal-prismatic cages to the electron-deficient nitroaromatics quenched the fluorescence emission of 3D cages, demonstrating that the "host" cages may be developed into selective and discriminatory fluorescent sensors for nitroaromatics.

We are confident that the efficient construction of 3D cages from preorganized metalloligands via coordination-driven self-assembly will open a door to new supramolecular nanoarchitectures with functional metallic centers. This will allow, for example, the expression of novel magnetic and photophysical properties, as well as catalytic behavior. Furthermore, self-assemblies of functional metalloligands may also find application in the fabrication of stimulus-responsive molecular devices.[8d]

Experimental Section

General Details. Metalloligands **2**,[8e] **10**, and **11**[11a,b] were prepared according to reported methods. **1** was synthesized using a procedure analogous to that of **2**. Deuterated solvents were purchased from Cambridge Isotope Laboratory (Andover, MA). NMR spectra were recorded on either a Varian Unity 300 MHz or a Bruker 300 MHz spectrometer. ^{1}H NMR chemical shifts are reported relative to residual solvent signals, and $^{31}P\{^1H\}$ NMR chemical shifts are referenced to an external unlocked sample of 85% H_3PO_4 (δ 0.0). Mass spectrometry spectra for the self-assemblies were recorded on a Micromass Quattro II triple-quadrupole mass spectrometer using electrospray ionization with a MassLynx operating system. Electronic absorption spectra were recorded on a Perkin-Elmer Lambda 750 UV−Vis spectrophotometer. Fluorescence emission studies were carried out on a Horiba Jobin Yvon Fluoromax-4 spectrometer. The solvents used for all photophysical studies were of spectroscopic grade and purchased from commercial sources. From a single crystal of **12**, the diffraction data were collected at 100 K on an ADSC Quantum 210 CCD diffractometer with synchrotron radiation (λ = 0.900 00 Å) at the Macromolecular Crystallography Beamline 6B1, Pohang Accelerator Laboratory, Pohang, Korea. The raw data were processed and scaled using the program *HKL2000*. The structure was solved by direct methods, and refinements were carried out with full-matrix least squares on F^2 with the appropriate software implemented in the *SHELXTL* program package.

Synthesis of Tris[1-(4-pyridyl)acetylacetonato]gallium (1). Sodium bicarbonate (197 mg, 2.35 mmol) was added to a solution of 4-pyridylbutane-1,3-dione (335 mg, 2.05 mmol) and $Ga(NO_3)_2$ (150 mg, 0.58 mmol) in methanol and water (10 mL; 1:1, v/v). After stirring at room temperature for 4 h, a white solid precipitated and was collected by filtration. The crude product was then dissolved in CH_2Cl_2, washed with water, dried over anhydrous sodium sulfate, and filtered, and the solvent was evaporated under reduced pressure. Then, an ethyl acetate and hexane mixture (20 mL; 1:1, v/v) was added to the residue, precipitating a white solid that was collected by filtration to afford **1** (168 mg). Yield: 52%. ^{1}H NMR [CD_2Cl_2/CD_3NO_2 (2:1, v/v), 300 MHz, 298 K]: δ 8.55 (m, 6H, H_α-Py), 7.63 (m, 6H, H_β-Py), 6.30 (dd, 3H, J = 3.3 Hz), 2.15 (m, 9H). Anal. Calcd for $C_{54}H_{48}Ga_2N_6O_{12}$: C, 58.30; H, 4.35; N 7.55. Found: C, 58.56; H, 4.26; N, 7.29.

Synthesis of the Trigonal-Bipyramidal Cage 5. A CD_2Cl_2 solution (0.60 mL) of **1** (2.18 mg, 3.92 μmol) was added dropwise to a CD_3NO_2 solution of **3** (4.29 mg, 5.88 μmol). The mixture was stirred at room temperature for 2 h before being transferred into the appropriate vessels for NMR or ESI-MS characterization. The solid product was obtained by removing the solvent in vacuo. Yield: 93%. $^{31}P\{^1H\}$ NMR [CD_2Cl_2/CD_3NO_2 (2:1, v/v), 121.4 MHz]: δ −1.4 (s, ^{195}Pt satellites, $^1J_{Pt-P}$ = 3059.2 Hz). ^{1}H NMR [CD_2Cl_2/CD_3NO_2 (2:1, v/v), 300 MHz, 298 K]: δ 8.91 (m, 12H, H_α-Py), 7.95, 7.90 (d, 12H, H_β-Py), 6.23 (s, 6H, enol-H), 2.16 (s, 18H, $-CH_3$), 1.65−1.75 (m, 36H, PCH_2CH_3), 1.15−1.25 (m, 54H, PCH_2CH_3). MS (ESI) for **5** ($C_{96}H_{138}F_{18}Ga_2N_6O_{30}P_6Pt_3S_6$): m/z 1500.2 ([M − 2OTf]$^{2+}$), 951.2 ([M − 3OTf]$^{3+}$). Anal. Calcd for $C_{96}H_{138}F_{18}Ga_2N_6O_{30}P_6Pt_3S_6$: C, 33.93; H, 4.21; N, 2.55. Found: C, 34.13; H, 4.50; N, 2.40.

Synthesis of the Trigonal-Bipyramidal Cage 6. A CD_2Cl_2 solution (0.60 mL) of tris[1-(4-pyridyl)acetylacetonato]aluminum(III) (**2**) (2.22 mg, 4.32 μmol) was added dropwise to a CD_3NO_2 solution of **3** (4.73 mg, 6.49 μmol). The mixture was stirred at room temperature for 2 h before being transferred into the appropriate vessels for NMR or ESI-MS characterization. The solid product was obtained by removing the solvent under vacuum. Yield: 96%. $^{31}P\{^1H\}$ NMR [CD_2Cl_2/CD_3NO_2 (2:1, v/v), 121.4 MHz]: δ −0.27 (s, ^{195}Pt satellites, $^1J_{Pt-P}$ = 3097.2 Hz). ^{1}H NMR [CD_2Cl_2/CD_3NO_2 (2:1, v/v), 300 MHz, 298 K]: δ 8.90 (m, 12H, H_α-Py), 7.72, 7.92 (d, 12H, H_β-Py), 6.35 (s, 6H, enol-H), 2.15 (s, 18H, $-CH_3$), 1.70 (m, 36H, PCH_2CH_3), 1.20 (m, 54H, PCH_2CH_3). MS (ESI) for **6** ($C_{96}H_{138}Al_2F_{18}N_6O_{30}P_6Pt_3S_6$): m/z 1457.8 ([M − 2OTf]$^{2+}$), 654.7 ([M − 4OTf]$^{4+}$). Anal. Calcd for $C_{96}H_{138}Al_2F_{18}N_6O_{30}P_6Pt_3S_6$: C, 34.86; H, 4.33; N, 2.61. Found: C, 34.63; H, 4.57; N, 2.44.

Synthesis of the Trigonal-Bipyramidal Cage 7. 1 (0.79 mg, 1.42 μmol) and the organoplatinum 60° acceptor **4** (2.48 mg, 2.13 μmol) were mixed in an acetone-d_6/D_2O (1:1, v/v) solution and kept at 65 °C for 12 h before being transferred into the appropriate vessels for NMR or ESI-MS characterization. The solid product was obtained by removing the solvent in vacuo. Yield: 90%. $^{31}P\{^1H\}$ NMR [acetone-d_6/D_2O (1:1, v/v), 121.4 MHz]: δ 14.5 (s, ^{195}Pt satellites, $^1J_{Pt-P}$ = 2670.8 Hz). ^{1}H NMR [acetone-d_6/D_2O (1:1, v/v), 300 MHz, 298 K]: δ 9.32 (m, 12H, H_α-Py), 8.82 (s, 6H), 8.42 (d, 12H, J = 6.3 Hz, H_β-Py), 7.97 (m, 6H), 7.85 (m, 12H), 5.70 (s, 6H), 2.55 (s, 18H, $-CH_3$), 2.35 (m, 72H, PCH_2CH_3), 1.35 (m, 108H, PCH_2CH_3). MS (ESI) for **7**

($C_{168}H_{252}Ga_2N_{12}O_{30}P_{12}Pt_6$): m/z 1445.8 ($[M - 3NO_3]^{3+}$), 1068.8 ($[M - 4NO_3]^{4+}$). Anal. Calcd for $C_{168}H_{252}Ga_2N_{12}O_{30}P_{12}Pt_6$: C, 43.85; H, 5.52; N, 3.65. Found: C, 43.96; H, 5.88; N, 3.41.

Synthesis of the Trigonal-Bipyramidal Cage 8. **2** (1.08 mg, 2.11 μmol) and the organoplatinum 60° acceptor **4** (3.67 mg, 3.16 μmol) were mixed in an acetone-d_6/D_2O (1:1, v/v) solution and kept at 65 °C for 12 h before being transferred into the appropriate vessels for NMR or ESI-MS characterization. The solid product was obtained by removing the solvent in vacuo. Yield: 92%. $^{31}P\{^1H\}$ NMR [acetone-d_6/D_2O (1:1, v/v), 121.4 MHz]: δ 11.8 (s, ^{195}Pt satellites, $^1J_{Pt-P}$ = 2658.7 Hz). ^{1}H NMR [acetone-d_6/D_2O (1:1, v/v), 300 MHz, 298 K]: δ 9.05 (m, 12H, H_α-Py), 8.55 (s, 6H), 8.12 (d, 12H, J = 6.3 Hz, H_β-Py), 7.70 (m, 6H), 7.56 (m, 12H), 5.40 (s, 6H), 2.26 (s, 18H, $-CH_3$), 1.52 (m, 72H, PCH_2CH_3), 1.15 (m, 108H, PCH_2CH_3). MS (ESI) for **8** ($C_{174}H_{252}Al_2N_{12}O_{30}P_{12}$): m/z 1473.4 ($[M - 3NO_3]^{3+}$), 1089.6 ($[M - 4NO_3]^{4+}$). Anal. Calcd for $C_{174}H_{252}Al_2N_{12}O_{30}P_{12}$: C, 43.68; H, 5.62; N, 3.72. Found: C, 43.66; H, 5.80; N, 3.52.

Synthesis of the Trigonal-Prismatic Cage 12. A CD_3NO_2 solution (0.5 mL) of the tripodal donor **9** (1.50 mg, 0.004 mmol) was added dropwise to a CD_3OD solution (0.5 mL) of ruthenium triflate acceptor **10** (5.15 mg, 0.006 mmol). The mixture was then stirred for 4 h at room temperature. Upon the addition of diethyl ether, a yellow crystalline powder was obtained. Yield: 89%. ^{1}H NMR (400 MHz, CD_3COCD_3): δ 8.21 (d, $^3J_{H,H}$ = 6.6 Hz, 12H, Py-H_α), 7.78 (s, 6H, Hbz), 7.61 (d, $^3J_{H,H}$ = 6.6 Hz, 12H, Py-H_β), 6.11 (d, $^3J_{H,H}$ = 6.3 Hz, 12H, Har), 5.96 (d, $^3J_{H,H}$ = 6.3 Hz, 12H, Har), 2.96 (sept, $^3J_{H,H}$ = 6.9 Hz, 6H, CH), 2.29 (s, 18H, CH_3), 1.39 (d, $^3J_{H,H}$ = 6.9 Hz, 36H, CH_3). MS (ESI) for **12** ($C_{126}H_{114}F_{18}N_6O_{30}Ru_6S_6$): 1517.0 ($[M - 2OTf]^{2+}$), 961.7 ($[M - 3OTf]^{3+}$). Anal. Calcd for $C_{126}H_{114}F_{18}N_6O_{30}Ru_6S_6$: C, 45.40; H, 3.45; N, 2.52. Found: C, 45.31; H, 3.41; N, 2.50.

Synthesis of the Trigonal-Prismatic Cage 13. A CD_3NO_2 solution (0.5 mL) of the tripodal donor **9** (2.63 mg, 0.007 mmol) was added dropwise to a CD_3OD solution (0.5 mL) of the acceptor **11** (9.37 mg, 0.010 mmol). The mixture was then stirred for 4 h at room temperature. Upon the addition of diethyl ether, a wine-red crystalline solid was formed and collected. Yield: 83%. ^{1}H NMR (400 MHz, CD_3COCD_3): δ 8.45 (d, $^3J_{H,H}$ = 6.6 Hz, 12H, Py-H_α), 7.84 (s, 6H, H-bz), 7.65 (d, $^3J_{H,H}$ = 6.6 Hz, 12H, Py-H_β), 6.21 (d, $^3J_{H,H}$ = 6.3 Hz, 12H, H_{Ar}), 6.01 (d, $^3J_{H,H}$ = 6.3 Hz, 12H, H_{Ar}), 5.81 (s, 6H, H_q), 3.01 (sept, $^3J_{H,H}$ = 6.92 Hz, 6H, CH), 2.26 (s, 18H, CH_3), 1.39 (d, $^3J_{H,H}$ = 6.9 Hz, 36H, CH_3). MS (ESI) for **13** ($C_{138}H_{120}F_{18}N_6O_{30}Ru_6S_6$): 1592.8 ($[M - 2OTf]^{2+}$), 1011.9 ($[M - 3OTf]^{3+}$). Anal. Calcd for $C_{138}H_{120}F_{18}N_6O_{30}Ru_6S_6$: C, 47.58; H, 3.47; N, 2.41. Found: C, 47.55; H, 3.44; N, 2.43.

Photophysical Studies of 12 and 13. Fluorescence quenching studies were performed by adding a stock methanol solution of TNT or PA (1.0×10^{-3} M) gradually to 2.0 mL of methanol solutions of **12** or **13** (1.0×10^{-6} M). The sample was excited at 280 nm and the emission intensity monitored at 350 nm. Analysis of the normalized fluorescence intensity (I_0/I) as a function of increasing quencher concentration ([G]) was well described by the Stern−Volmer equation $I_0/I = 1 + K_{SV}[G]$. K_{SV} was calculated by fitting the equation to the Stern−Volmer plot.

Acknowledgment. P.J.S. thanks the NIH (Grant GM-057052) for financial support. V.V. and K.-W.C. appreciate the financial support of WCU program (R33-2008-000-10003) of the National Research Foundation of Korea and the Pohang Accelerator Laboratory (PAL) for X-ray structural analysis. P.S.M. thanks the DST, India for financial support.

Supporting Information Available: ^{1}H and $^{31}P\{^1H\}$ NMR spectra of trigonal-bipyramidal cages **6**−**8**, ESI-MS spectra for cages **7** and **8**, ^{1}H NMR spectra of **12** and **13**, spectral and photophysical data of **12** and **13** in methanol, and crystallographic file (in CIF format) of **12**. This material is available free of charge via the Internet at http://pubs.acs.org.